LASER
& PHOTONICS
REVIEWS

Laser Photonics Rev. **11,** No. 2, 1700005 (2017) / **DOI** 10.1002/lpor.201700005

LETTER
ARTICLE

Abstract A mid-infrared (MIR) supercontinuum (SC) has been demonstrated in a low-loss telluride glass fiber. The double-cladding fiber, fabricated using a novel extrusion method, exhibits excellent transmission at 8–14 μm: $<$ 10 dB/m in the range of 8–13.5 μm and 6 dB/m at 11 μm. Launched intense ultrashort pulsed with a central wavelength of 7 μm, the step-index fiber generates a MIR SC spanning from ~2.0 μm to 16 μm, for a 40-dB spectral flatness. This is a fresh experimental demonstration to reveal that telluride glass fiber can emit across the all MIR molecular fingerprint region, which is of key importance for applications such as diagnostics, gas sensing, and greenhouse CO_2 detection.

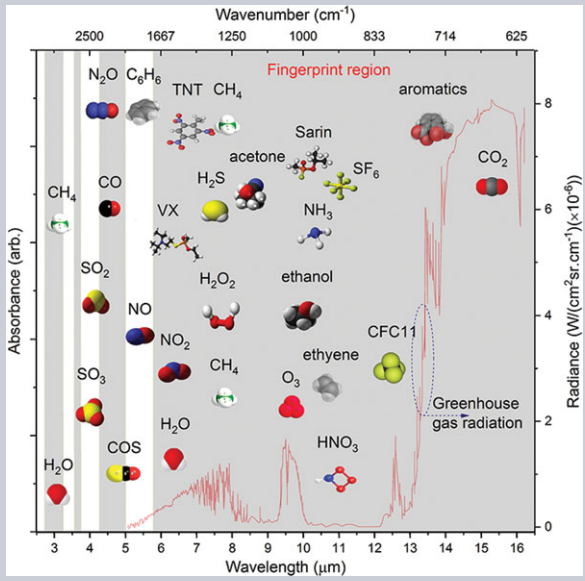

Mid-infrared supercontinuum covering 2.0–16 μm in a low-loss telluride single-mode fiber

Zheming Zhao[1,2,3,], Bo Wu[1,3,**], Xunsi Wang[1,3,*], Zhanghao Pan[1,3], Zijun Liu[1,3], Peiqing Zhang[1,3], Xiang Shen[1,3], Qiuhua Nie[1,3], Shixun Dai[1,3,*], and Rongping Wang[1,3,4,*]**

1. Introduction

The MIR (2–16 μm) spectral region is of great importance because most molecules display of fundamental vibrational absorption located in this region, leaving distinctive spectral fingerprints [1], which can also be adopt to track the scent of the greenhouse gases, CO_2, CH_4 and others in monitoring global warming. High-quality light sources with spatial coherence, broad bandwidth and high brightness are needed to meet the MIR applications. Supercontinuum is considered an ideal source for various applications, such as fluorescence microscopy, optical coherence tomography and spectroscopy [2]. However, it is extremely important to extend the SC spectrum into the MIR region in order to develop various applications in the MIR. For example, the fundamental vibrations of different molecules are located at a so-called molecular fingerprint region from 3 to 16 μm. A strong coherent light source covering this wavelength range is essential to develop spectral tools to detect these molecules [3]. Obviously, this requires the materials with excellent transparency in the MIR, and only Te-based bulk glasses have the ability to transmit from near-IR up to 25 μm [4, 5], and possess the potential of fiber transparency up to 16 μm. Moreover, Te-based chalcogenide (ChG) glasses have the maximal nonlinear refractive index [6] among all glasses, making them ideal for MIR SC generation.

Recently, many ultrabroadband MIR SCs have been demonstrated in traditional (non-Te-based) ChG fibers [7–9]. Experimental work on SC generation in ChG fibers was initially focused on As–S and As–Se [8–12], in which ultrabroadband SCs were generated via pumping in the anomalous dispersion regime in step-index ChG fibers. For example, SC spectra with a long-wavelength edge up to

[1] Laboratory of Infrared Material and Devices, The Research Institute of Advanced Technologies, College of Information Science and Engineering, Ningbo University, Ningbo, 315211, China
[2] Nanhu College, Jiaxing University, Jiaxing, 314001, China
[3] Key Laboratory of Photoelectric Materials and Devices of Zhejiang Province, Ningbo, 315211, China
[4] Centre for Ultrahigh bandwidth Devices for Optical Systems, Laser Physics Centre, Research School of Physics and Engineering, The Australian National University, Canberra, ACT 2600, Australia
**Zheming Zhao and Bo Wu contributed equally to this work.
*Corresponding author: e-mail: xunsiwang@siom.ac.cn; daishixun@nbu.edu.cn; wangrongping@nbu.edu.cn

13.3 μm were demonstrated in a $Ge_{10}As_{23.4}Se_{66.6}/As_2Se_3$ step-index fiber pumped with 100-fs pulses at 6.3 μm [7], and a MIR SC covering the 2.0–15.1 μm region were reported in a 3-cm long $As_2Se_3/AsSe_2$ fiber pumped in the anomalous dispersion regime [9]. Several ternary materials like GeAsSe and GeSbSe were also employed for SC generation [13, 14]. It is well known that replacement of a lighter element by a heavier one, can enhance the optical nonlinearity of the materials [15], and extend the transparency to longer wavelengths [16], and thus is beneficial to SC generation. Therefore, telluride glasses are expected to have the highest optical nonlinearity and broadest transmission window [16]. Recently, we have demonstrated a broad SC spectrum in a Ge–As–Se–Te step-index fiber pumped in the normal dispersion regime [17]. However, the broadening of SC spectra to longer wavelengths was limited by the multiphonon absorption of Se–Se. Previous work has demonstrated the potentials for far-infrared (FIR) applications in Ge–Ga–Te [5], Ge–Te–I [16], and Ge–Te–AgI [18, 19] glass systems without containing Se. Iodine can trap free electrons from tellurium and help to form more stable glasses [16]. Moreover, the high atomic weight of "iodine", which is a neighbor of tellurium in the periodic table, allows the low phonon character of the glass matrix to be maintained and the far-IR transparency to be retained, while providing improved rheological properties. Also, it has been shown that the nonlinearity of ChG glasses could be enhanced when doping with Cu or Ag [20], hence the Ge–Te–AgI glass system was chosen for fiber drawing and SC generation in this work. However, in reference [19], the single-index fiber with an exorbitant loss (25 dB/m at 11 μm) was far from fit for SC generation and other applications. The cause of the inefficiency is that the Te-based glasses are not stable enough towards crystallization in the preparation of structured fibers by traditional fiber fabrication methods.

In this work, we report the fabrication of Ge–Te–AgI fiber with double-cladding structure and its SC generation in MIR. The fiber drawn from extruded preform exhibits excellent transmission at 8–14 μm: $<$ 10 dB/m in the range of 8–13.5 μm and 6 dB/m at 11 μm. A broad MIR SC spanning from $\sim$2.0 up to 16.0 μm, for a 40-dB spectral flatness, can be achieved by pumping the fiber in the normal dispersion regime at 7 μm.

2. Experimental section

Glass and fiber fabrication: The chalcohalide glasses were synthesized by the conventional melt-quenching method. 5N elements were employed as starting materials in order to obtain high-purity glasses. Ge and Te were further purified using a distillation method containing Mg to remove oxide impurities. The double-cladding fiber was fabricated using a preform-drawing process. The preform with a core-cladding ratio of 1:2 was coextruded by a 9-mm core glass rod along with a 26-mm cladding glass rod [21]. Then, the structured preform with a ratio of 1:5 was coextruded again by a 46-mm $Ge_{10}Sb_{10}Se_{80}$ glass rod to obtain a small-core fiber. The fiber was drawn in a home-made drawing tower with N_2 protection, and the drawing temperature was 210 °C.

Characterization: The glass-transition temperature (T_g) and the onset crystallization temperature (T_x) were analyzed by differential scanning calorimetry (DSC). The refractive indices of the glasses were measured by an IR ellipsometer (IR-VASE MARK II, J.A. Woollam Co.), and the dispersion of the fundamental mode (FM) was calculated using a commercial software (RSOFT).

Fiber loss measurement: The fiber loss was measured with a Fourier transform infrared (FTIR) spectrometer (Nicolet 5700) using the cut-back method. A 1.2-m long fiber was employed to evaluate the attenuation. By removing 40-cm pieces of the fiber using a precision fiber optic cleaver (FK11-LDF, Photon kinetics, Inc.), each cleave was observed by the optical microscope (Keyence, VHX-1000) to ensure a sufficiently flat interface. The attenuation was calculated by Loss $= 10^{*}\log(P_1/P_2)/L$, (where P_1 is the input power, P_2 is the output power, and L is the removed length of fiber.) .

SC generation: The pump laser was an optical parametric amplifier (OPA) system and the details were described in reference [17]. The MIR pulses ($\sim$150 fs, repetition rate of 1 kHz) were launched into a 14 cm of Ge–Te–AgI fiber using ZnSe lens. The output beam from the fiber was injected into a monochromator directly. To remove the gases such as O_2, H_2O and CO_2, nitrogen gases were introduced to fill the monochromator. The liquid nitrogen cooled mercury cadmium telluride (HgCdTe) detector (spectral response range: 1–16 μm) was used to detect SC signals that were amplified by a lock-in amplifier. To eliminate high-order signal, long-pass filters (1.9, 3.6, 7.0 and 11.0 μm) were applied as order-sorting filters.

3. Results and discussion

With the help of differential scanning calorimetry (DSC), the thermal stabilities of the core and cladding glasses were recorded, which indicate their T_g are all about 145–150 °C, and T_x are about 225–230 °C. Here, ΔT, the difference between T_x and T_g, a criterion for glass stability, is usually *more than 100 °C at least for* fiber drawing. However, the ΔT of core glass $(Ge_{10}Te_{43})_{90}$-AgI_{10} and cladding glass $(Ge_{10}Te_{40})_{90}$-AgI_{10} are all around 80 °C, and it is challenging to draw high-quality fiber. Thus, no fiber with core–cladding structure based on chalcohalide material had been demonstrated. Here, we employed a coextrusion method to successfully prepare $(Ge_{10}Te_{43})_{90}$-AgI_{10} / $(Ge_{10}Te_{40})_{90}$-AgI_{10} / $Ge_{10}Sb_{10}Se_{80}$ preform, and the corresponding fiber were successfully drawn for the first time via a careful control of the drawing temperature. Measurements of the refractive indices of the core and cladding glasses together with the calculated NA are shown in Fig. 1a. The transmission spectrum of the fiber we achieved is shown in Fig. 2a where the transparent edge is extended over 12 μm, easily

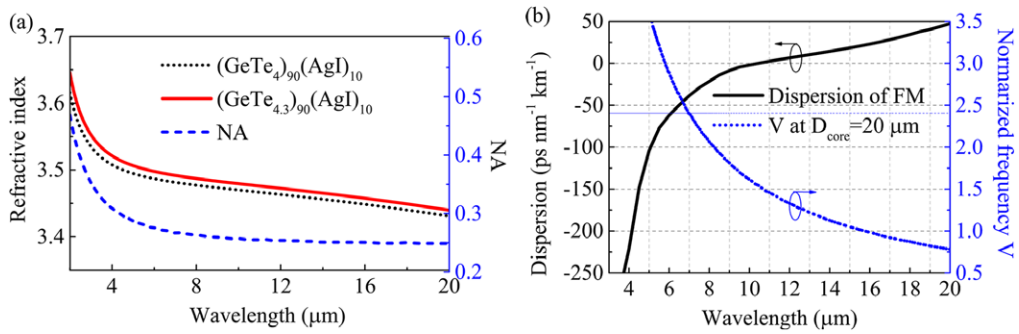

Figure 1 (a) Measured refractive indices of the glasses and the calculated NA; (b) Calculated *V* and dispersion (FM).

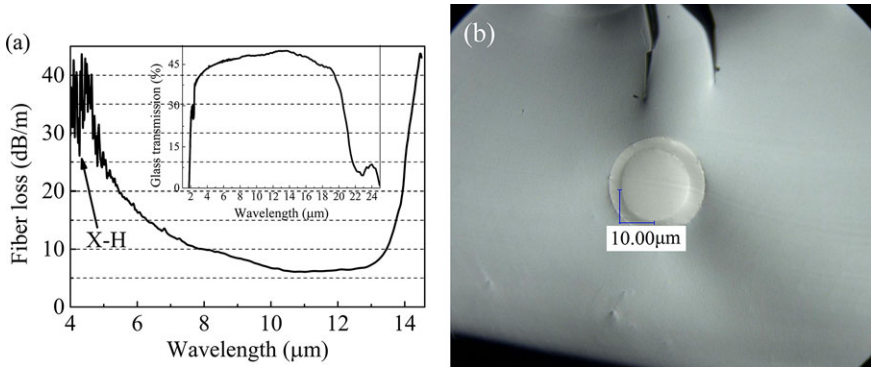

Figure 2 (a) Measured optical loss in the fiber, inserted with a transmission of bulk core glass; (b) The cross-sectional image of the fiber (2000×).

up to 14.5 μm. By pumping a 14-cm long fiber at 7 μm with a 150-fs pulse at a repetition rate of 1 kHz, a MIR SC spectrum spanning from ~2.0 to 16 μm was generated.

The step-index fiber had a $(Ge_{10}Te_{43})_{90}$-AgI_{10} core with a diameter of 20 μm and two claddings: the first is $(Ge_{10}Te_{40})_{90}$-AgI_{10} and the second is $Ge_{10}Sb_{10}Se_{80}$, as shown in Fig. 2b. It is well known that a double-cladding or even multicladding layer can be used in the design of dispersion-shifted fiber based on the glasses with similar optical properties. Nevertheless, in this work the second cladding of a Ge–Sb–Se layer was only employed as a "jacket" to protect the iodine-contained glass from easy deliquescence in air. In addition, such a Ge–Sb–Se protective layer can slim down the core size and improve the robustness of fiber preform extrusion with more thermostability. The normalized frequency *V* of this fiber is obtained from:

$$V = \frac{\pi D_{\text{Core}}}{\lambda}\sqrt{n_{\text{core}}^2 - n_{\text{clad}}^2} = \frac{\pi D_{\text{Core}}}{\lambda}\text{NA}, \qquad (1)$$

where D_{core} is the core diameter and λ is the propagating light wavelength. Due to the small difference of refractive indices and the small core, the fiber works at single-mode when the wavelength is larger than 7 μm, while $V \leq 2.405$, as shown in Fig. 1b. The zero-dispersion wavelength (ZDW) of the fiber is about 10.5 μm. The optical loss of the fiber was presented in Fig. 2a, where the inset was the transmission of the core glass with a thickness of 5 mm. No obvious impurity absorption peaks can be observed in the loss spectrum except the X–H contaminant absorption (X means Te, Ge or other elements) at around 4.25 μm. The vibration at shorter wavelength is due to the photoenergy-gap absorption. The loss spectrum going up rapidly after 14 μm is due to multiphonon absorption. This fiber exhibits excellent transmission at 8–14 μm: < 10 dB/m in the range of 8–13.5 μm and 6 dB/m at 11 μm, respectively. To the best of our knowledge, this is a fairly low loss in any entirely Te-based ChG optical fiber (without Se or other glass-network former). However, the fiber loss need to be reduced in the future, or the fiber length must be reduced and allow the transmitting waveband to expand as wide as the bulk glass (thickness of 5 mm), just shown in the insert of Fig. 2a. Since the output power from an optical parametric amplifier (OPA) at a wavelength beyond 10 μm is too low to be used as a pumping source, it is impossible to pump a Te-based ChG fiber at ZDW. Considering the optical spectra of the fiber and the pump power from difference frequency generation (DFG), a short wavelength of 7 μm was chosen to pump the fiber for SC generation.

The experimental SC spectra excited by different pumping wavelengths: (a) 6 μm (b) 7 μm (c) 8 μm, are shown in Fig. 3 in the normal dispersion regime. The mean power in the label is the pulse power out from OPA. We observed that when the pump power increased, the spectrum quickly broadened and crossed the ZDW easily. For example, when the fiber was pumped at 6 μm, far from the ZDW, the spectra became broad with increasing pump power, and the broadest SC spectrum from 2.4 to 14.5 μm at 40 dB could be achieved under 14 mW pump power, the spectra bandwidth is 5.6–8.7 μm at 10 dB, 3.1–10.8 μm at 20 dB, 2.8–12.7 μm at 30 dB, as shown in Fig. 3a. When pumping at 7 μm, the SC generation under lower pump power

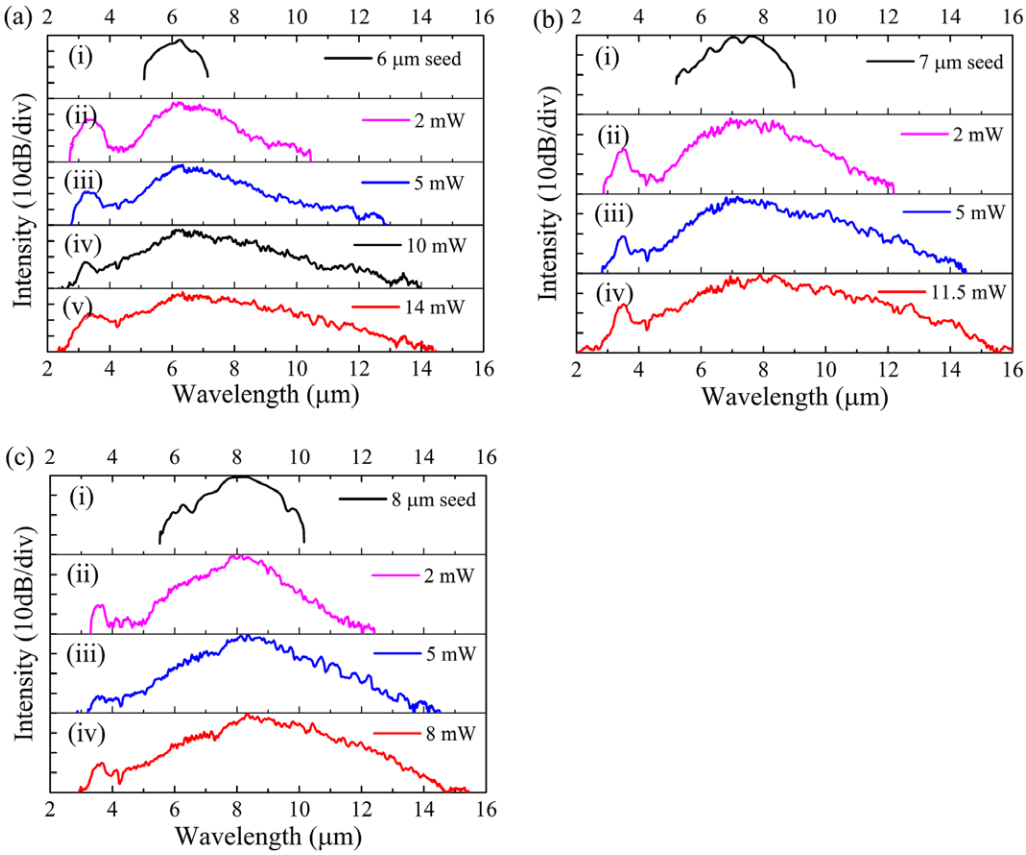

Figure 3 Experimental SC spectra pumped at: (a) 6 μm (b) 7 μm (c) 8 μm; the mean power in the label is the pulse power out from OPA.

Table 1 Experimental MIR SC generation in the ChG fiber (more than 12 μm)

Fiber	Fiber length (cm)	ZDW (μm)	Pump wavelength (μm)	SC bandwidth (μm)	Reference
As–Se	8.5	5.83	6.3	1.4–13.3 (30 dB)	[7]
As–Se	3	5.5	9.8	2–15.1 (–)	[9]
Ge–Sb–Se	20	5.5	6	1.8–14 (–)	[13]
Ge–As–Se–Te	23	10.5	4.5	1.5–14 (30 dB)	[17]
Ge–Te–AgI	14	10.5	7	2–16 (40 dB)	This work

(2 mW) is mostly limited to the normal dispersion regime. As the pump power increases (> 5 mW), high-order Raman lines are generated and soliton formation is induced by the third-order Raman line in the anomalous dispersion regime [22], so the SC spans across the ZDW and causes significantly red-shift as far as to 16 μm at 40 dB, and the position with maximum intensity in the spectrum shifts to ~8.0 μm, the spectra bandwidth is 6–10.5 μm at 10 dB, 4.8–12.9 μm at 20 dB, 3–14.5 μm at 30 dB, as shown in Fig. 3b(iv). On further increasing the pump wavelength to 8 μm, the SC spectrum becomes slightly narrow from ~3.0 to 15.4 μm at 40 dB under 8 mW laser power, the spectra bandwidth is 7.45–10.7 μm at 10 dB, 5.7–12.5 μm at 20 dB, 3.3–13.8 μm at 30 dB, as shown in Fig. 3c(iv). The SC spectra can be extended to 14.5 μm, 16 μm and 15.4 μm under maximum pump power at different pump wavelengths of 6, 7, and 8 μm, respectively.

It is well known that when pumping in the normal dispersion regime, the pulses initially endure strong self-phase modulation (SPM), and could result in optical-wave breaking (OWB) due to self-steepening and third-order dispersion, and finally causes a significant shift of the spectrum both in the blue and in red. In all cases, the dip at around 4.25 μm in the spectra is caused by the X–H contaminant absorption, which is identical to the loss of the fiber. Comparing the SC spanning spectra pumped at different wavelength it was found that 7 μm and 8 μm are more efficient than 6 μm as the pump wavelength in this fiber. On the other hand, the spectral extension with the 7-μm pump wavelength at maximum power was found

to be longer simply because of the more intense pump power.

Table 1 lists the experimental SC results generated in the different ChG fibers, broadband SC can be obtained by pumping in the anomalous dispersion regime in Se-based ChG fiber as well as in the normal dispersion regime in Te-based fiber. It was found that Te-based fibers have a much larger transparent window and ZDW than any other ChG fiber. Generally, the coherence property of SC pumped in the normal dispersion regime is better than that pumped in the anomalous dispersion regime. Therefore, we believe Te-based fibers are more suitable for highly coherent SC generation in MIR.

4. Conclusions and outlook

In summary, we have fabricated a low-loss telluride step-index fiber by a novel extrusion method. To the best of our knowledge, the Te-based double-cladding fiber had not been reported before. The fiber exhibits excellent transmission in the atmospheric window of 8–14 μm: < 10 dB/m in the range of 8–13.5 μm and 6 dB/m at 11 μm, respectively. We have investigated the SC generation of the fiber pumped by different laser wavelengths and powers in the normal dispersion regime. A SC spectrum covering 2.0–16 μm for a 40-dB spectral flatness can be obtained by pumping the fiber at 7 μm in the normal dispersion regime. This fiber-based SC can cover the CO_2 molecule region located around 4.25 μm and 15 μm. Such a broad SC source has great potential to be used in various applications, especially for complex biomolecule spectroscopic analysis and greenhouse gases monitoring in all MIR (2–16 μm).

Acknowledgements. We thank Dr. Xing Li and Changgui Lin for enlightened discussion. This work was funded by National Natural Science Foundation of China (NSFC) (61435009, 61377099, 61627815, 61307060); the Opened Key–Subject Construction Fund of Zhejiang Province, China (xkxl1508, xkxl1318); the Program for New Century Excellent Talents in University of Ministry of Education of China (NCET-10-0976); the 151 Talents and 1000 Talents Plan in Zhejiang Province, China; the K. C. Wong Magna Fund of Ningbo University, China, and the Key Project of Nanhu College, Jiaxing University, China.

Received: 6 January 2017, **Revised:** 1 March 2017,
Accepted: 6 March 2017

Published online:

Key words: nonlinear materials, mid-IR supercontinuum, low-loss telluride fiber, fingerprint region.

References

[1] A. Schliesser, N. Picque, and T. W. Haensch, Nature Photon. **6**, 440–449 (2012).
[2] G. Steinmeyer and J. S. Skibina, Nature Photon. **8**, 814–815 (2014).
[3] G. A. Mark, Meas. Sci. Technol. **9**, 545 (1998).
[4] V. Q. Nguyen, J. S. Sanghera, I. D. Aggarwal, and I. K. Lloyd, J. Am. Ceram. Soc. **83**, 855–859 (2000).
[5] S. Danto, P. Houizot, C. Boussard-Pledel, X. H. Zhang, F. Smektala, and J. Lucas, Adv. Funct. Mater. **16**, 1847–1852 (2006).
[6] B. J. Eggleton, B. Luther-Davies, and K. Richardson, Nature Photon. **5**, 141–148 (2011).
[7] C. R. Petersen, U. Moller, I. Kubat, B. Zhou, S. Dupont, J. Ramsay, T. Benson, S. Sujecki, N. Abdel-Moneim, Z. Tang, D. Furniss, A. Seddon, and O. Bang, Nature Photon. **8**, 830–834 (2014).
[8] F. Theberge, N. Thire, J. F. Daigle, P. Mathieu, B. E. Schmidt, Y. Messaddeq, R. Vallee, and F. Legare, Opt. Lett. **39**, 6474–6477 (2014).
[9] T. Cheng, K. Nagasaka, T. H. Tuan, X. Xue, M. Matsumoto, H. Tezuka, T. Suzuki, and Y. Ohishi, Opt. Lett. **41**, 2117–2120 (2016).
[10] R. R. Gattass, L. B. Shaw, V. Q. Nguyen, P. C. Pureza, I. D. Aggarwal, and J. S. Sanghera, Opt. Fiber Technol. **18**, 345–348 (2012).
[11] U. Møller, Y. Yu, I. Kubat, C. R. Petersen, X. Gai, L. Brilland, D. Méchin, C. Caillaud, J. Troles, B. Luther-Davies, and O. Bang, Opt. Express **23**, 3282–3291 (2015).
[12] C. R. Petersen, P. M. Moselund, C. Petersen, U. Møller, and O. Bang, Opt. Express **24**, 749–758 (2016).
[13] H. Ou, S. Dai, P. Zhang, Z. Liu, X. Wang, F. Chen, H. Xu, B. Luo, Y. Huang, and R. Wang, Opt. Lett. **41**, 3201–3204 (2016).
[14] Y. Yu, B. Zhang, X. Gai, C. Zhai, S. Qi, W. Guo, Z. Yang, R. Wang, D.-Y. Choi, S. Madden, and B. Luther-Davies, Opt. Lett. **40**, 1081–1084 (2015).
[15] T. Wang, X. Gai, W. Wei, R. Wang, Z. Yang, X. Shen, S. Madden, and B. Luther-Davies, Opt. Mater. Express **4**, 1011–1022 (2014).
[16] A. A. Wilhelm, C. Boussard-Pledel, Q. Coulombier, J. Lucas, B. Bureau, and P. Lucas, Adv. Mater. **19**, 3796–3800 (2007).
[17] Z. Zhao, X. Wang, S. Dai, Z. Pan, S. Liu, L. Sun, P. Zhang, Z. Liu, Q. Nie, X. Shen, and R. Wang, Opt. Lett. **41**, 5222–5225 (2016).
[18] X. Wang, Q. Nie, G. Wang, J. Sun, B. Song, S. Dai, X. Zhang, B. Bureau, C. Boussard, C. Conseil, and H. Ma, Spectrochim. Acta. A Mol. Biomol. Spectrosc. **86**, 586–589 (2012).
[19] C. Conseil, J. C. Bastien, C. Boussard-Pledel, X. H. Zhang, P. Lucas, S. X. Dai, J. Lucas, and B. Bureau, Opt. Mater. Express **2**, 1470–1477 (2012).
[20] K. Ogusu and K. Shinkawa, Opt. Express **17**, 8165–8172 (2009).
[21] C. Jiang, X. S. Wang, M. M. Zhu, H. J. Xu, Q. H. Nie, S. X. Dai, G. M. Tao, X. Shen, C. Cheng, Q. D. Zhu, F. X. Liao, P. Q. Zhang, P. Q. Zhang, Z. J. Liu, and X. H. Zhang, Opt. Eng. **55**, 056114 (2016).
[22] U. Moller and O. Bang, Electron. Lett. **49**, 63–65 (2013).

